Cold Regions Science and Technology xxx (xxxx) xxx–xxx

Contents lists available at ScienceDirect

Cold Regions Science and Technology

journal homepage: www.elsevier.com/locate/coldregions

Analysis of the hazard caused by ice avalanches from the hanging glacier on the Eiger west face

Stefan Margreth[a,*], Martin Funk[b], Daniel Tobler[c], Pierre Dalban[c], Lorenz Meier[d], Juerg Lauper[e]

[a] WSL Institute for Snow and Avalanche Research SLF, Davos, Switzerland
[b] Laboratory of Hydraulics, Hydrology and Glaciology (VAW), ETH Zurich, Zurich, Switzerland
[c] GEOTEST AG, Zollikofen, Switzerland
[d] GEOPRAEVENT AG, Zurich, Switzerland
[e] Jungfrau Railways, Interlaken, Switzerland

ARTICLE INFO

Keywords:
Risk management
Ice avalanche
Avalanche simulation
Hazard assessment

ABSTRACT

The Eiger hanging glacier is located in the west face of the Eiger in the Bernese Alps (Switzerland). Large ice avalanches, especially if they trigger secondary snow avalanches, endanger parts of the Jungfrau ski area and the Jungfraujoch railway. The latter leads to the Jungfraujoch, one of the top tourist destinations in Europe. The formation of a crevasse immediately behind the front of the hanging glacier was detected in autumn 2015, indicating an impending icefall with a maximum ice volume of 80,000 m^3. Consequently, a hazard analysis was performed for four different scenarios with varying ice volumes and snow conditions. The analysis showed that a 100 m high rocky ridge situated in the main flow direction of the avalanches plays a crucial role due to its braking and deflecting effect. Closure plans were prepared for the four scenarios investigated. The railway station is especially endangered in the extreme scenario assuming an ice volume of 80,000 m^3 and unstable snow conditions. We therefore recommended to trigger avalanches below the hanging glacier artificially after snowfall events and to install an early warning and alarm system to minimize the closure times for the railway and ski area.

1. Introduction

The Eiger hanging glacier is located on the west face of the Eiger in the Bernese Alps (Switzerland). The hanging glacier is a so-called avalanching glacier (Pralong and Funk, 2006) located on a sufficiently steep slope to allow detaching ice chunks (calving) to fall from the glacier terminus and give rise to ice avalanches (Fig. 1). The glacier extends from 3500 to 3200 m a.s.l. with a surface slope of 20° at the terminus. The front of the glacier is 200 m wide and 30 m high (Fig. 2). Ice lamellas with typical volumes of < 10,000 m^3 break off periodically (Fig. 3). Large ice avalanches, especially if they trigger secondary snow avalanches, endanger parts of the ski area Jungfrau and the railway, which runs through a 7 km long tunnel through the Eiger to the Jungfraujoch. The railway was opened in 1912. The Jungfraujoch located at 3454 m a.s.l. is one of the top tourist destinations in Europe and has one million visitors yearly. On peak days, up to 5000 visitors use the railway. The area around the railway station Eigergletscher is particularly exposed. The hanging glacier has been monitored with an automatic camera since 1996. The formation of a crevasse immediately behind the front was detected in autumn 2015, indicating an impending failure with a maximum ice volume of 80,000 m^3.

2. Topographical and avalanche situation

Ice avalanches breaking off the hanging glacier first flow over 400 vertical meters through a 45° steep and 100 m wide gully. The gully is interrupted by small cliffs, which additionally favour the formation of powder snow avalanches. Below the steep channel, the topography widens onto a 35° slope with a surface area of 90,000 m^2. This is the main release area where ice avalanches can trigger secondary snow avalanches. Additional release areas for snow avalanches exist in the steep rock faces of the Eiger and Klein Eiger, which are separated from the main avalanche path by rocky ridges below the hanging glacier (Fig. 1). These release zones are rather wind exposed and snow is often blown off. During snowfall or warming periods loose snow avalanches are released, which disturb and stabilize the snowpack in the main release area for secondary snow avalanches. The rocky Rotstock ridge, situated in the main flow direction of the avalanches, plays a crucial role due to its braking and deflecting effect (Figs. 4 and 5). The elevation of the ridge above the surrounding terrain varies between 55 and

* Corresponding author at: WSL Institute for Snow and Avalanche Research SLF, Flüelastrasse 11, CH 7260 Davos Dorf, Switzerland.
E-mail address: margreth@slf.ch (S. Margreth).

http://dx.doi.org/10.1016/j.coldregions.2017.05.012
Received 28 November 2016; Received in revised form 21 April 2017; Accepted 29 May 2017

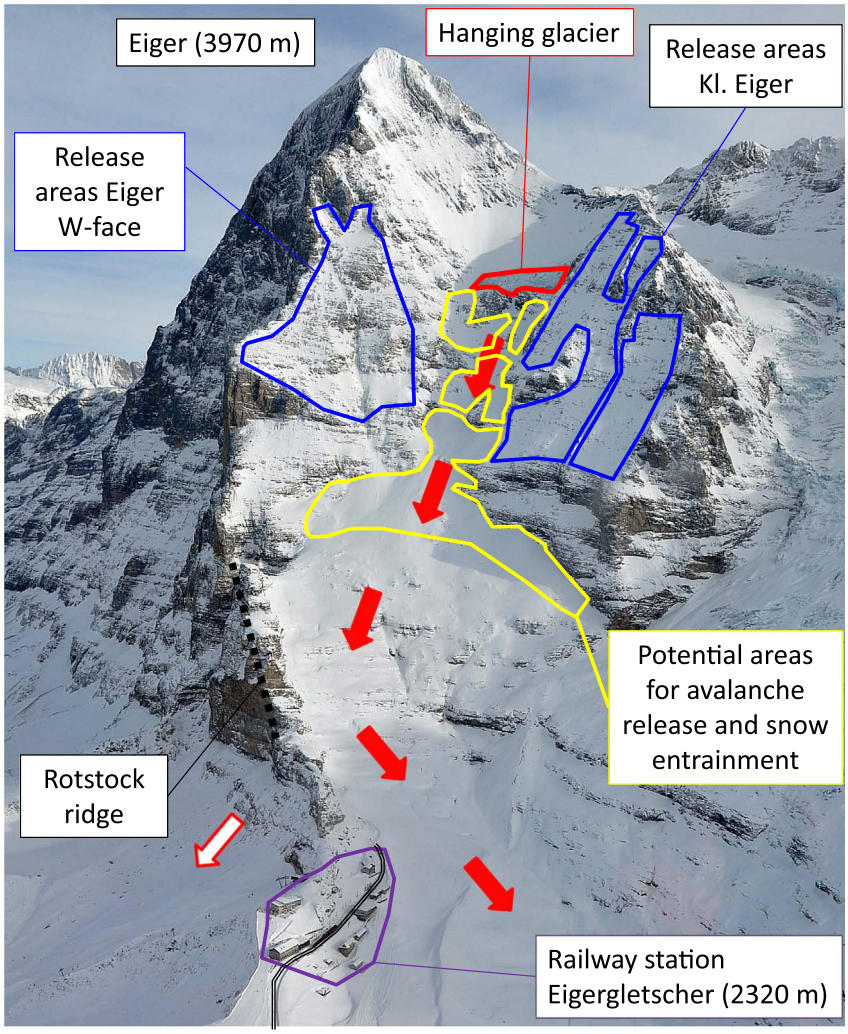

Fig. 1. Overview on the Eiger with the hanging glacier in the W-face, possible flow paths of ice avalanches and location of the Eigergletscher railway station.

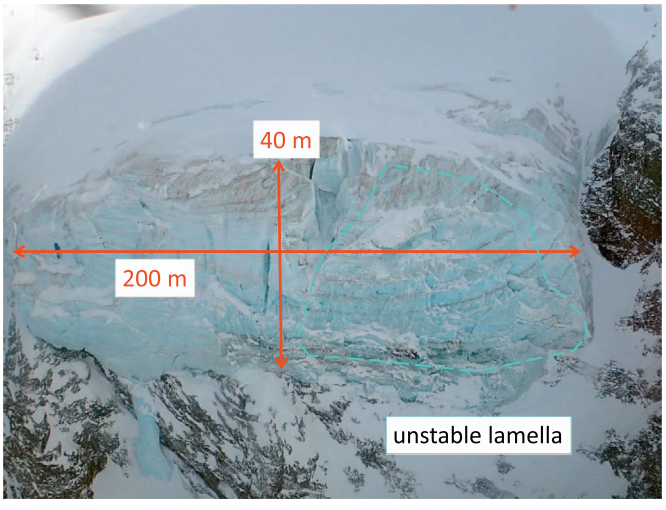

Fig. 2. Front of hanging glacier on Eiger W-face (18 January 2016).

110 m in the main impact zone. The ridge deflects avalanches southwestwards towards a glacial depression. In the absence of the rocky Rotstock ridge avalanches would flow straight on northwards. The railway station Eigergletscher situated at 2200 m a.s.l. is at the northern margin of the flow path of ice avalanches from the hanging glacier.

3. Glaciological situation

The surface area of the Eiger hanging glacier is 0.08 km^2 (Huss and Fischer, 2016) with a mean and maximum thickness of about 40 m and 70 m, respectively. The average ice velocity at the glacier front reaches 7 m a^{-1} (Lüthi and Funk, 1997). With a front area of ca. 6,000 m^2, the yearly ice flux amounts to 40,000 m^3 a^{-1}. The frontal zone is constantly supplied by ice from the glacier upstream and the ice-release volumes (40,000 m^3 a^{-1} on average) are small (~1%) compared with the total glacier volume (3 Mio m^3). Fracture at the front occurs because there is a cliff in front of the glacier. This topographic discontinuity limits the extension of the glacier and leads to calving when ice is transferred beyond this point. When calving occurs, the glacier margin forms an ice cliff. The unstable mass is an ice lamella, which breaks off from the glacier edge (Fig. 3). The typical ice-release volume is 1,000–100,000 m^3. In 1990, a large crevasse was observed behind the glacier front, indicating an impending breaking-off. It is well known that the velocity of unstable ice masses increases as a power law function of time prior to failure. This characteristic acceleration presents a finite-time singularity at the theoretical time of failure and it can be used to forecast the time of breaking off (Pralong et al., 2005). Based on measured surface velocities on the unstable part of the glacier performed during the early stage of the instability, an icefall of 100,000 m^3 of ice could be successfully predicted. The icefall occurred on 20 August 1990, three days after the predicted date (Pralong and Funk, 2006).

The Eiger hanging glacier is temperate, except in the vicinity of its front (Lüthi and Funk, 1997, Fig. 6). Lüthi and Funk (1997) argued that

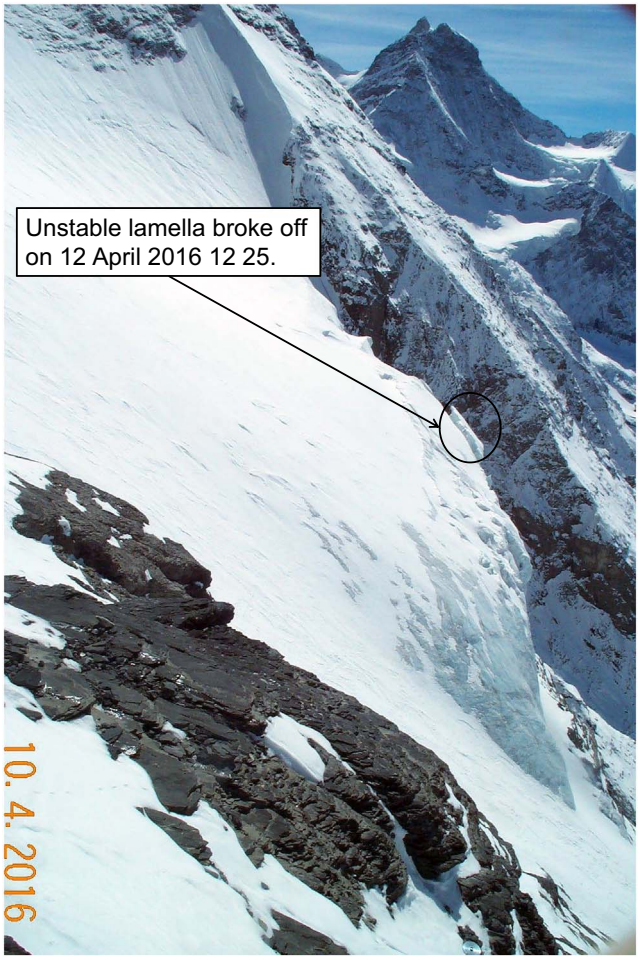

Fig. 3. Lateral view of the hanging glacier on Eiger W-face on 10 April 2016. The small ice lamella broke off on 12 April 2016, 12 25 (automatic camera VAW/ETHZ).

the temperature distribution may affect the global stability of the glacier, so that warming of the cold front due to climate change could destabilize a large part of the glacier. According to Faillettaz et al. (2015), the Eiger hanging glacier belongs to the category of avalanching glaciers that are partly frozen onto their bedrock with the

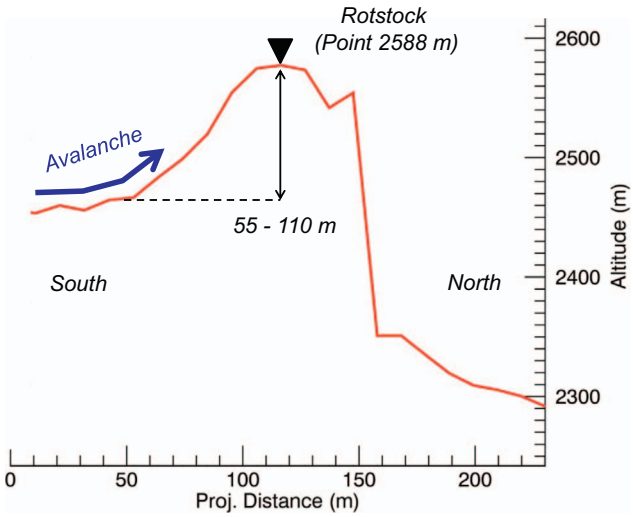

Fig. 5. Cross section of the Rotstock ridge.

presence of a temperate zone (indicating a transition state between a cold and temperate regime). In this case, the rupture would occur directly on the bedrock in the temperate area and could possibly propagate through the ice. Water at the ice/bedrock interface plays a key role in the initiation and the development of the instability and greatly complicates the glacier behavior. The presence of meltwater trapped within the glacier affects the extent of the temperate zone by release of latent energy produced when water freezes and may lead to the expansion of a weakly connected temperate zone at the interface between the glacier and its bedrock (Faillettaz et al., 2011). Successive hot summers could potentially warm the still frozen ice/bedrock interface, resulting in a reduction of the basal support. The presence of meltwater at the ice/bedrock interface also reduces the basal shear resistance, promoting the onset of the instability. This could affect the stability of a major part of the glacier and cause ice break-off volumes significantly larger than 100,000 m^3. The resulting instability can occur without clear precursory signs (Faillettaz et al., 2011). In this case, the only way to detect the initiation of the instability is to monitor the temporal and spatial evolution of the temperate zone at the interface. Numerical modeling including heat transfer and ice flow modeling is required to assess the contribution of the different heat sources and accurately

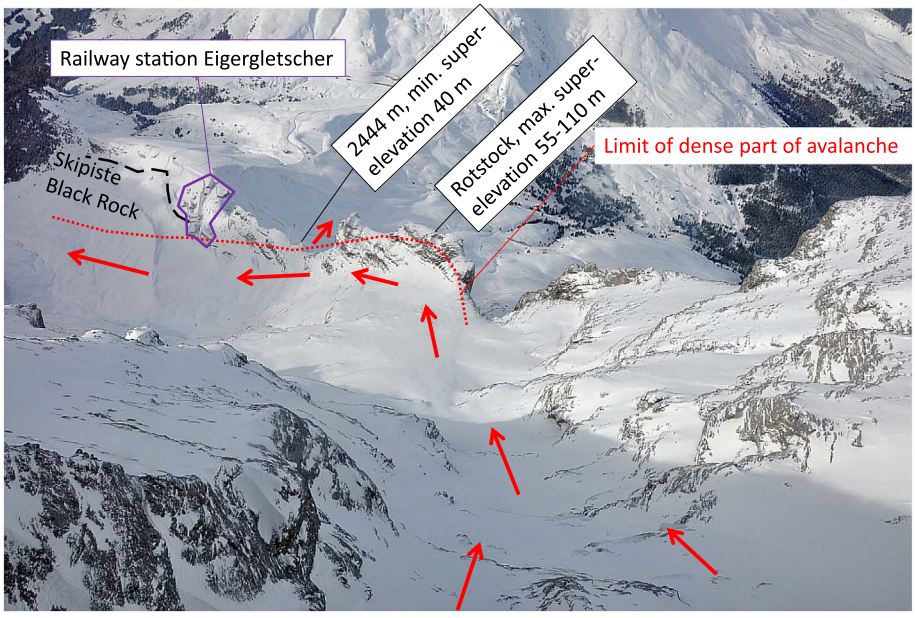

Fig. 4. View from hanging glacier along flow path with the Rotstock ridge.

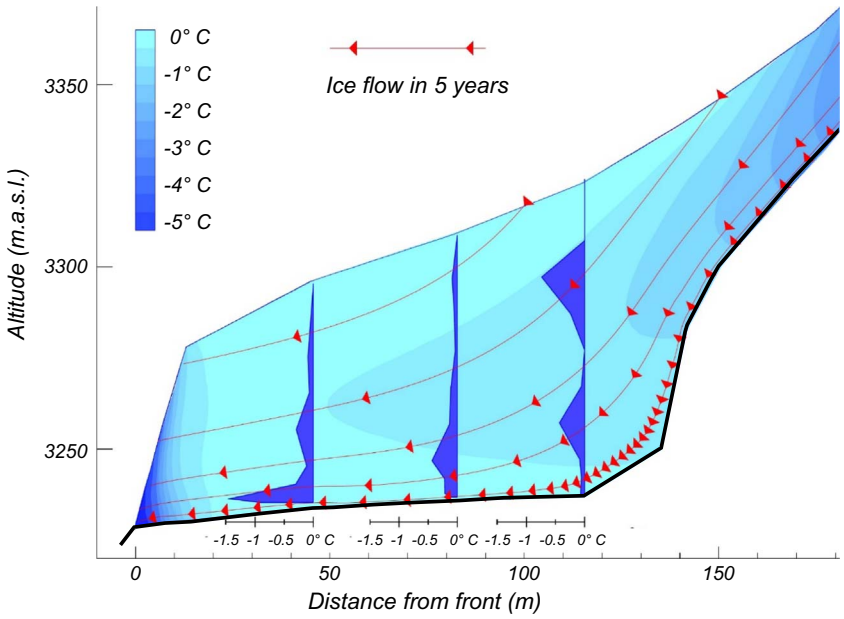

Fig. 6. 2D section of Eiger hanging glacier upstream of the glacier front (left margin). Results from a coupled ice flow/temperature model. Measured englacial ice temperatures in three boreholes are also shown (adapted from Lüthi and Funk, 1997).

Table 1
Overview of the investigated icefall scenarios.

Scenario	Ice volume	Entrainment volume	Suspension ratio	Average height of powder cloud	Zone of influence of core	Max. impact pressure powder cloud at railway station
1	10,000 m^3	–	14%	22 m	300 m above railway station	< 0.5 kPa
2	10,000 m^3	50,000 m^3	12%	37 m	80 m S of railway station	10–0.5 kPa
3	80,000 m^3	–	11%	32 m	20 m S of railway station	10–0.5 kPa
4	80,000 m^3	125,000 m^3	14%	53 m	Strikes the railway station	100–7 kPa

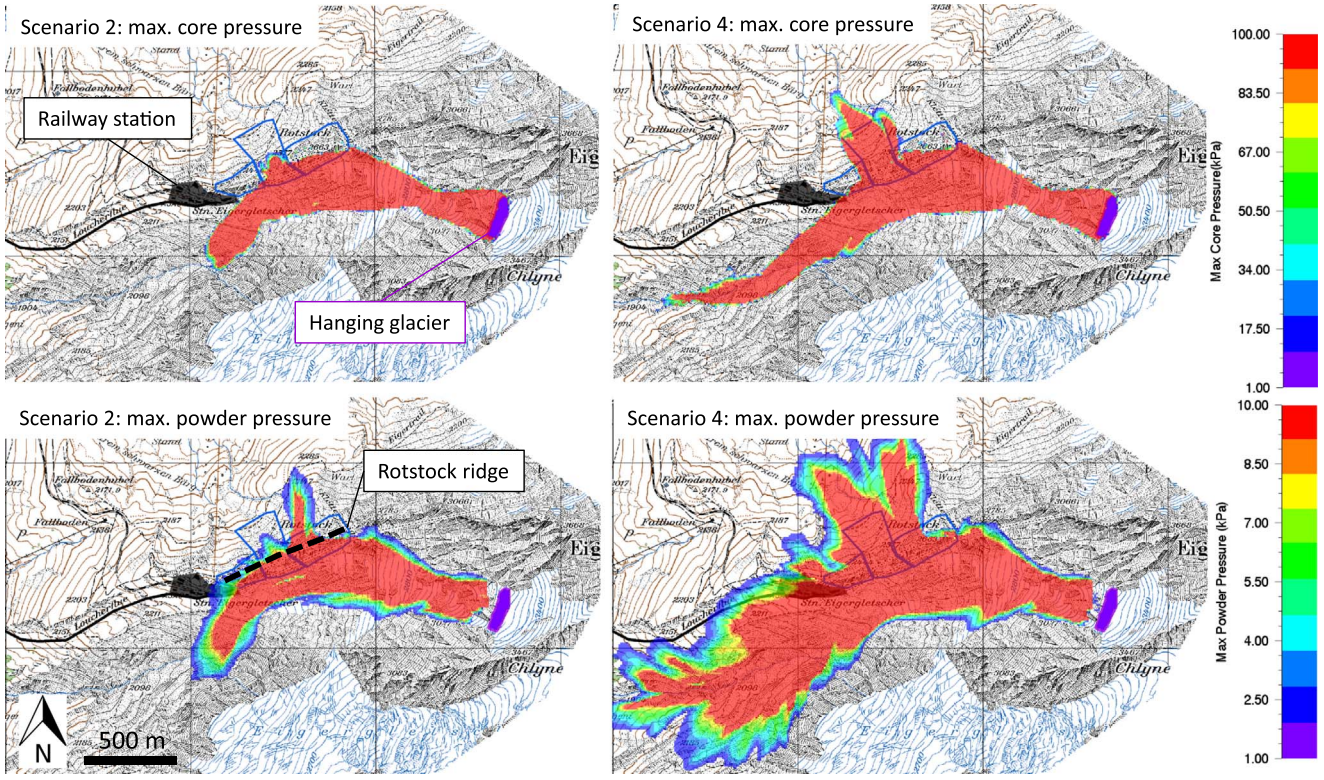

Fig. 7. Results of the RAMMS simulations for the scenarios 2 and 4. The top pictures show the maximal avalanche core pressure and the bottom pictures show the maximal powder pressure.

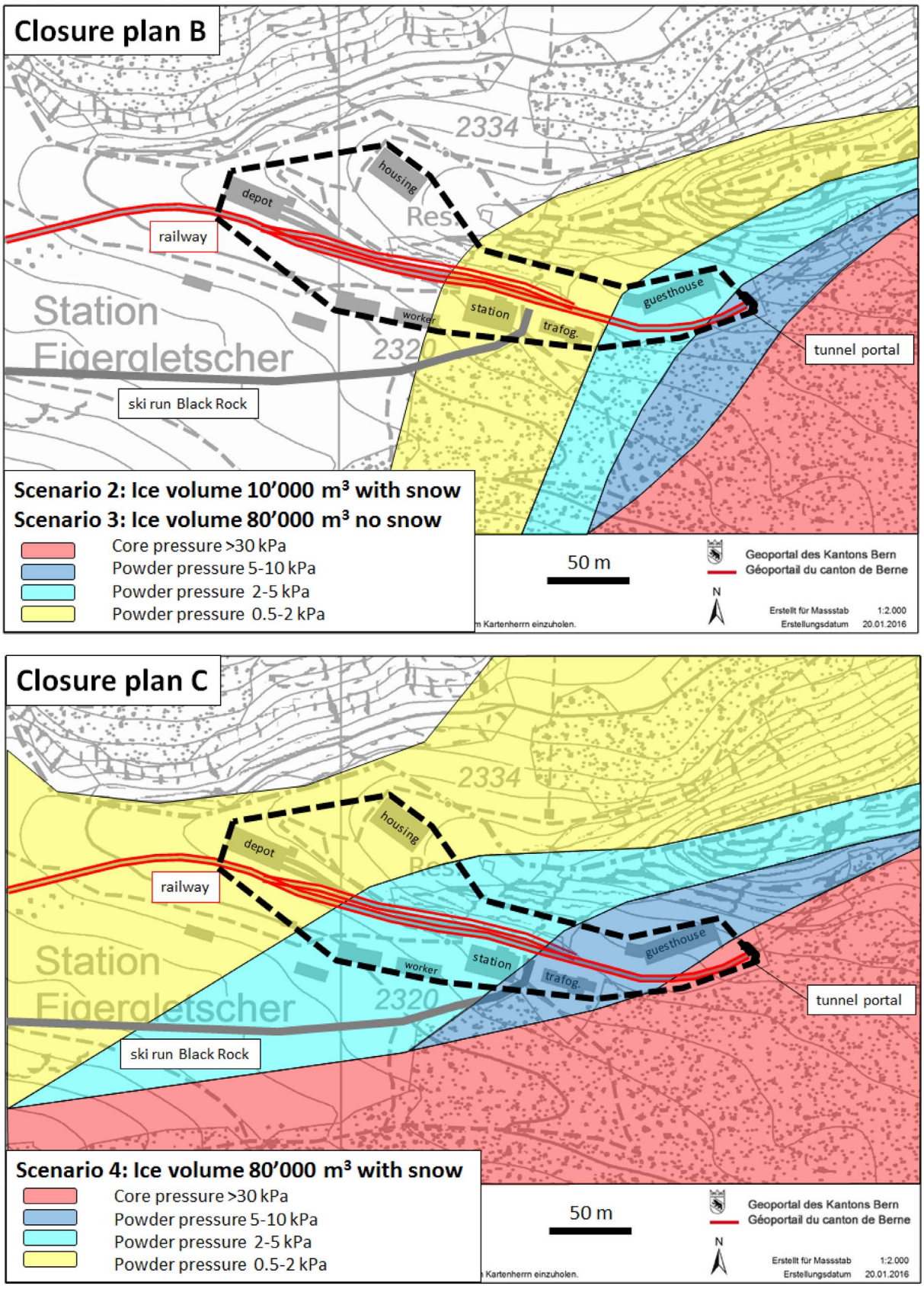

Fig. 8. Closure plans B and C with pressure zones for the area of the railway station Eigergletscher.

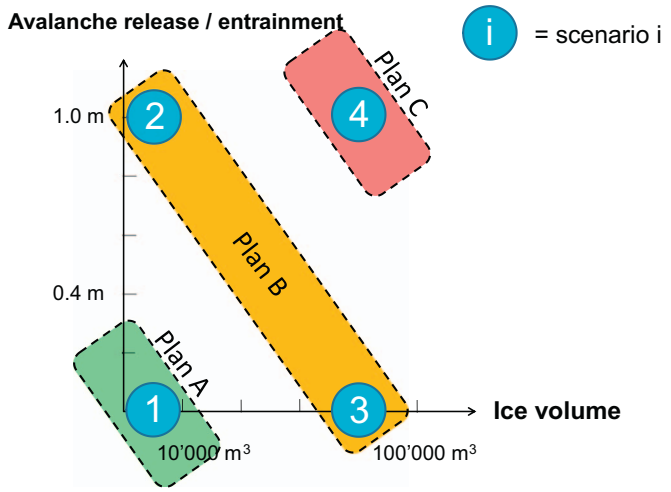

Fig. 9. Schematic diagram of the relation of the closure plans to the four investigated scenarios, which depend on the ice volume and the potential entrainment value.

simulate the ice temperature changes (Lüthi and Funk, 1997; Gilbert et al., 2014). Detecting the transition from a cold to a temperate bedrock using either experimental or numerical studies is the only way to assess the stability of the glacier.

4. Historical ice avalanches and investigated ice fall scenarios

The record of historical icefalls from the Eiger hanging glacier is incomplete, especially before 1980. We assume that ice avalanches smaller than 10,000 m^3 often went unnoticed. Larger ice avalanches were observed in 1982, 1990 and 1991 (Raymond et al., 2003). The summer 1990 event involved an ice volume of approximately 100,000 m^3 and is the largest documented icefall from the Eiger hanging glacier (Pralong and Funk, 2006). The ice avalanche missed the area of the railway station Eigergletscher by 65 m. Since the construction of the railway in 1898 it is unlikely that a large ice avalanche occurred in winter time, releasing additional snow masses. Such a large avalanche would likely have caused damage to the railway infrastructure. However, no such damage has been documented. Only minor damage, such as broken windows has occurred at the railway station. During this period of 117 years, the thickness of the hanging glacier has decreased slightly but the geometry of the glacier front has not changed much. The detachment of the whole hanging glacier with an ice volume of over 1 Mio m^3 is considered to be unlikely in the near future because the hanging glacier is currently frozen to the bedrock. In our study we evaluated the following four scenarios:

1. Icefall of 10,000 m^3 without snow entrainment (summer and winter with stable snowpack)
2. Icefall of 10,000 m^3 with snow entrainment (winter with unstable snowpack)
3. Icefall of 80,000 m^3 without snow entrainment (summer and winter with stable snowpack)
4. Icefall of 80,000 m^3 with snow entrainment (winter with unstable snowpack).

5. Avalanche dynamics calculations

The simulation of ice avalanches falling from a hanging glacier is complex. In summer with a snow free topography, the detaching ice mass is broken into smaller pieces of ice and forms a dense avalanche. Because of the steep topography, the formation of a powder cloud is likely, especially for large ice volumes. If the topography is snow covered, the ice avalanche can entrain part of the snow cover or release secondary snow avalanches and will be delayed by lower friction forces. Consequently, a combined snow/ice avalanche has a greater mass, an increased powder part and a longer runout.

We applied the two-layer RAMMS-RKE model which has been implemented in the research version of the RAMMS avalanche dynamics program (Christen et al., 2010). The two layer model consists of an avalanche core and a powder cloud. The cloud is treated as an inertial flow arising from the avalanche core (Bartelt et al., 2016). The density of the core is not constant - allowing dilute, dispersed and dense flows. The core of the avalanche is driven by the gravitational acceleration in the slope-parallel direction. The mass exchanges in the mixed flowing avalanche system are snow entrainment into the avalanche core, volume and mass blowout of ice-dust from the core into the powder cloud and direct air entrainment. The shearing in the core is considered with a Voellmy-type ansatz where the Coulomb friction μ and turbulent friction ξ depend on the configurational energy content of the core (Bartelt et al., 2016) implying that the friction values μ and ξ are adjusted to variations in the flow density. Central to the model equations is the inclusion of the free mechanical energy of the avalanche core which is the sum of the energy of the random granule motions and density changes (Buser and Bartelt, 2015). The model parameter α describes the production rate of the free mechanical energy in relation to the rate of work carried out by shear forces. The kinetic energy part is

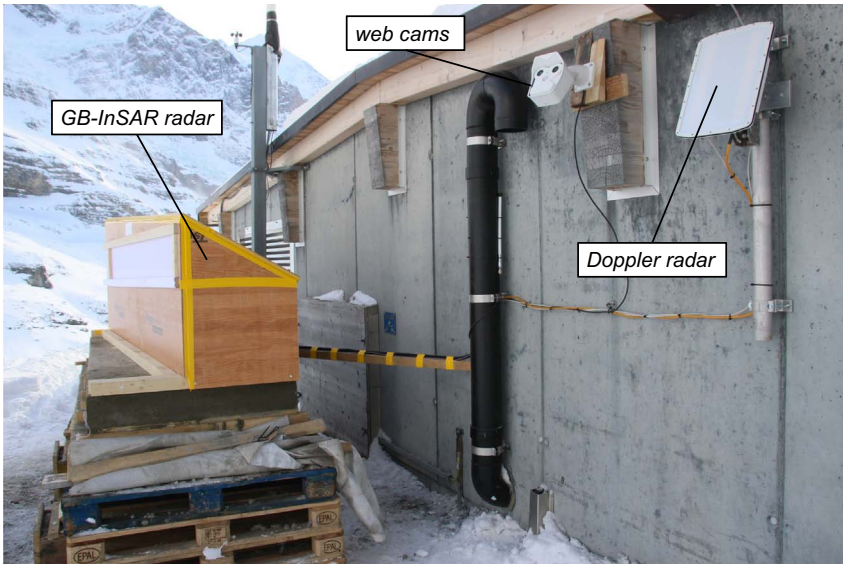

Fig. 10. The monitoring system installed at the railway station Eigergletscher consists of a GB-InSAR, Doppler radar and several webcams. The GB-InSAR is well protected in a wooden box.

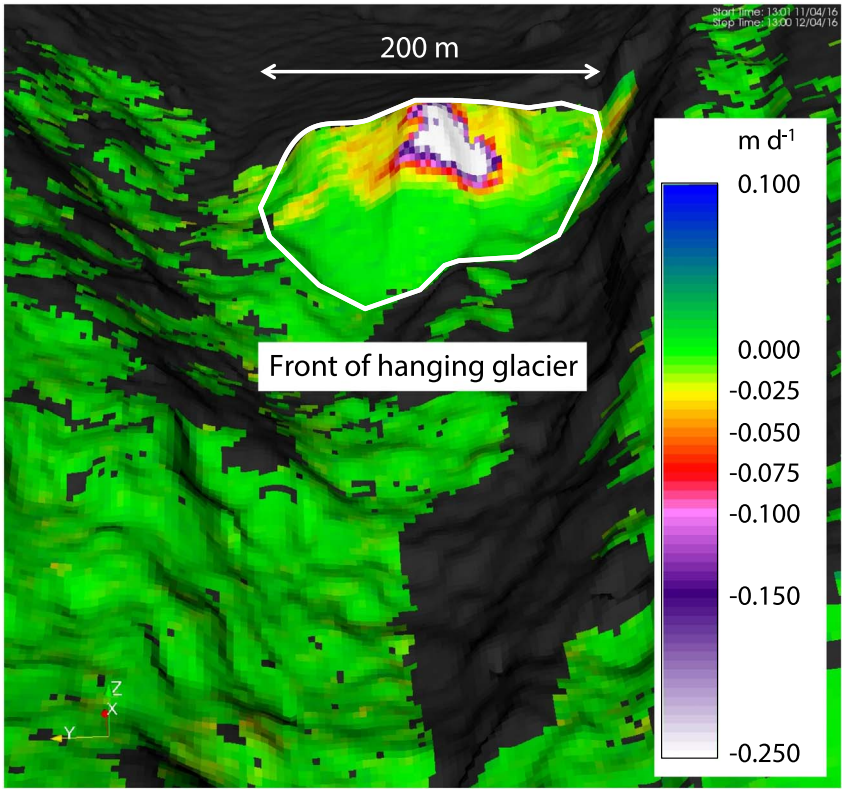

Fig. 11. Surface flow velocities (m d^{-1}) measured by the GB-InSAR and projected onto a digital elevation model. On 12 April 2016, the velocities at the front of the hanging glacier were higher than 0.25 m d^{-1}. The front of the hanging glacier shown with the white line has a width of 200 m and the active area has a surface of around 200 m^2.

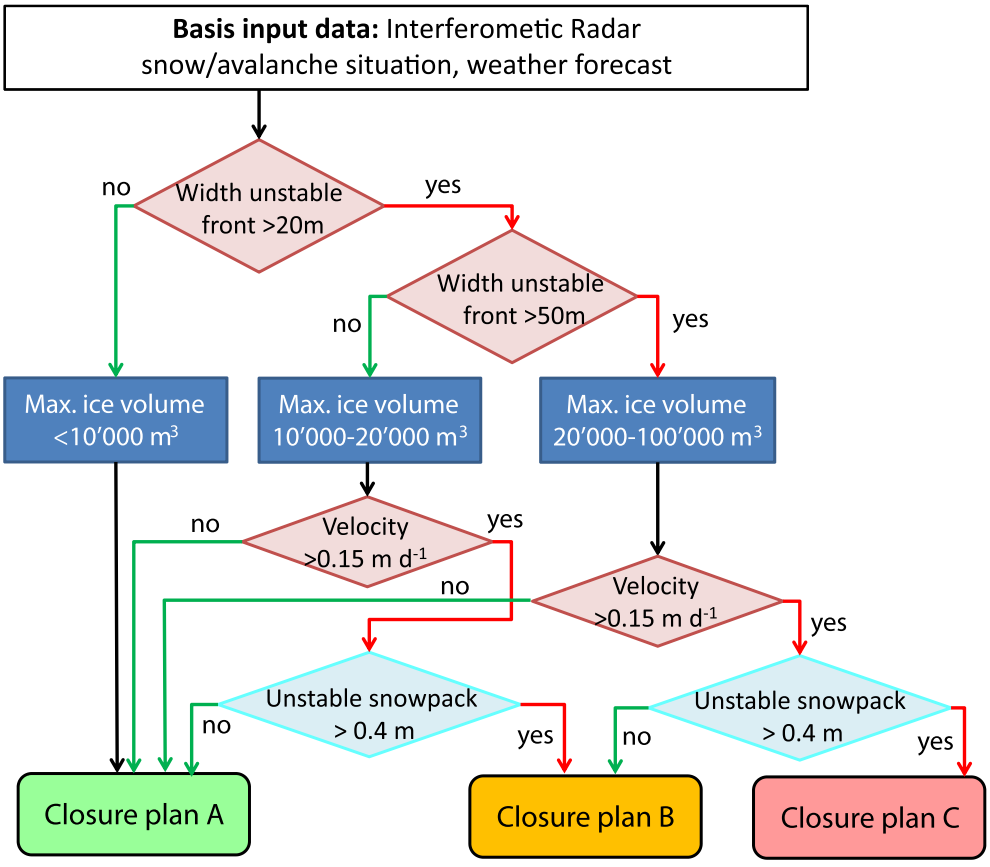

Fig. 12. Decision tree to determine the required closure plan in relation to the maximal ice volume, surface velocity and snowpack stability.

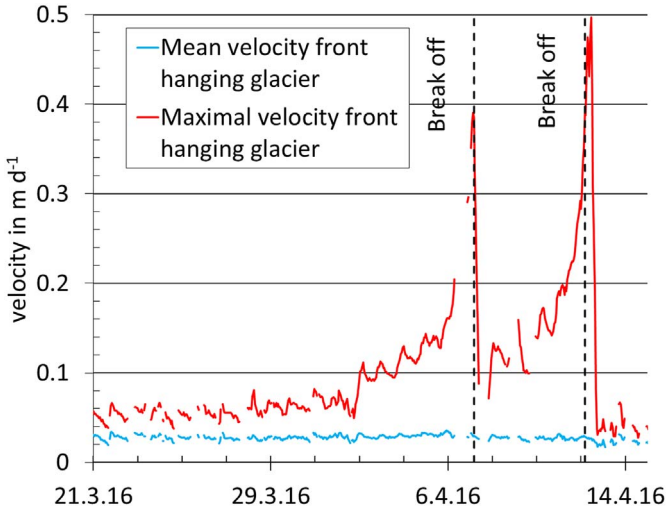

Fig. 13. Mean and maximal velocities at the front of the hanging glacier between 21 March 2016 and 14 April 2016 measured with the GB-InSAR. A distinct increase in velocity was observed prior to the two break-off events. Another icefall was recognized on 3 March 2016.

considered with the parameter β, which is highly dependent on the snow temperature. We applied the parameters $\alpha = 0.06$ and $\beta = 0.8$ in the simulations. For the avalanche core at rest we used a density $\rho_0 = 850\ \mathrm{kg\ m^{-3}}$, $\mu_0 = 0.55$, $\xi_0 = 2000\ \mathrm{m\ s^{-2}}$ and an ice temperature of $-10\ ^{\circ}\mathrm{C}$. These parameters were chosen on the basis of the simulation of the ice avalanche that struck the Everest base camp in Nepal on 25 April 2015 (Bartelt et al., 2016).

A large source of uncertainty in the simulation is the treatment of ice avalanches flowing over a snowpack. Observations show that if the snowpack is very stable the avalanche flows over the snowpack without entraining significant snow masses. If the snowpack is unstable, a secondary slab avalanche can be triggered and, if the snowpack is loose, the avalanche entrains snow. We approached this problem with the RAMMS entrainment module (Christen et al., 2010; Margreth et al., 2011). In scenarios 2 and 4, we assumed a potential entrainment height of 1.0 m, a snow density of $200\ \mathrm{kg\ m^{-3}}$ and a snow temperature of $-5\ ^{\circ}\mathrm{C}$ along the whole track of the avalanche. We used the velocity driven entrainment law implemented in RAMMS with an entrainment coefficient $k = 0.5$. This value defines the intake rate of snow by the ice avalanche. A value $k > 0.2$ ensures that snow is primarily taken in at the front of the avalanche, facilitating the formation of the powder cloud. In the simulations, the powder avalanche forms quickly after the release and the ice-avalanche core entrains practically the whole snowpack along the entire path.

The computational grid was generated from a Digital Elevation Model with a 2 m resolution. The simulation resolution is 10 m. First simulations showed that the braking and deflecting effect of the Rotstock ridge is not satisfactorily included in the model. Most of the avalanching snow flowed over the rocky ridge. We would expect a clear flow separation, according to our experience with other avalanche paths with a similar topography. We think that the powder cloud partly overflows the rocky ridge and that the core is deflected south-westwards. In order to respect this model deficiency, we introduced an area of increased friction along the rocky ridge ($\mu = 1.0$ instead of 0.55 and $\xi = 100$ instead of $2000\ \mathrm{m\ s^{-2}}$). These friction parameters are not physics-based but were chosen based on expert judgment to compensate for the underestimation of the effect of the rocky ridge in the simulations. An example of such an effect would be momentum loss due to the impact of the avalanche on the steep lateral rock face. The

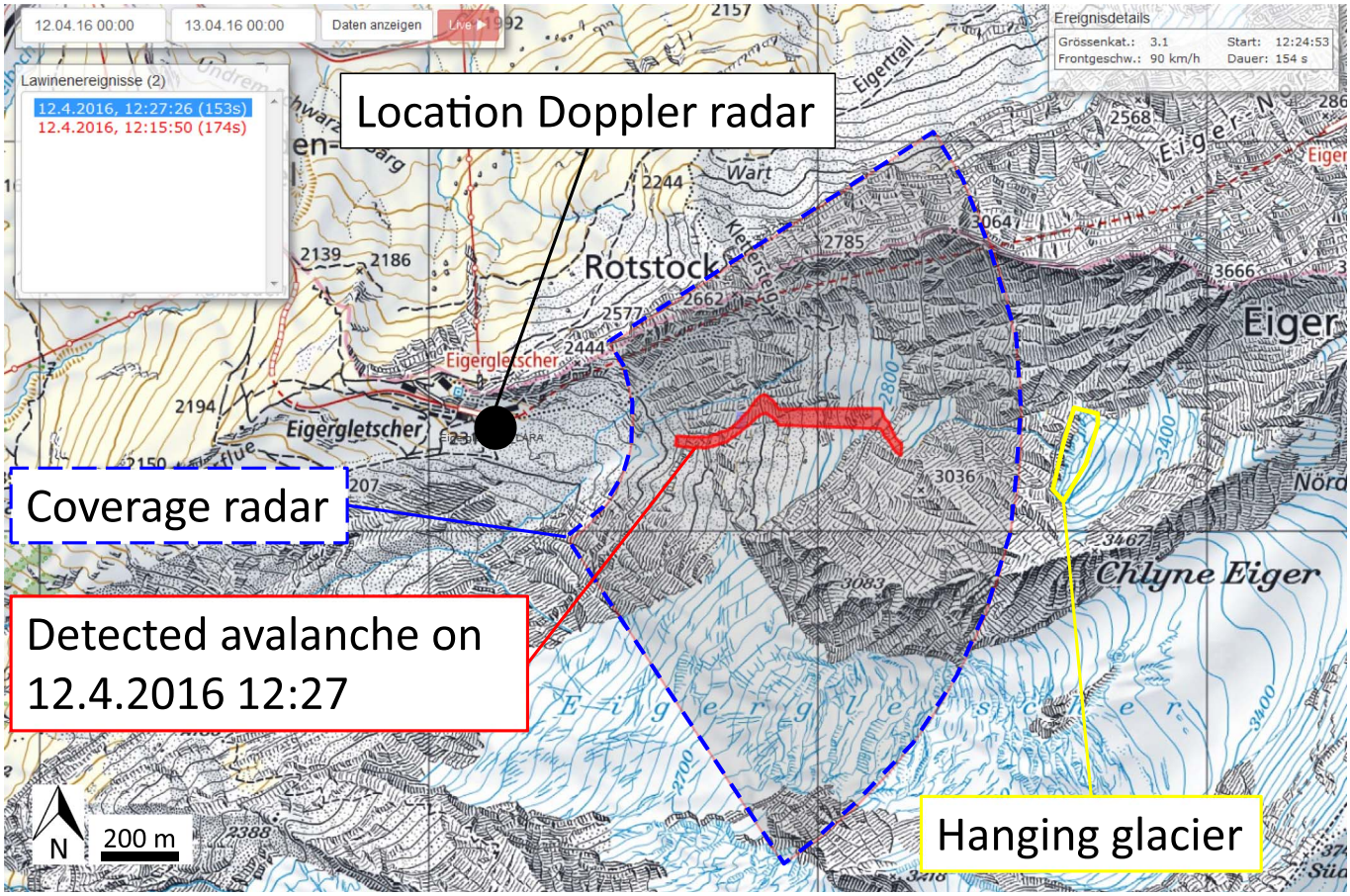

Fig. 14. GEOPRAEVENT online data portal with detected avalanche on 12 April 2016 and location of Doppler radar.

adapted friction parameters decelerate the avalanche and increase the deflecting effect of the rocky ridge.

The RAMMS simulations show the following results (Table 1):

- In **scenario 1** an ice avalanche with a volume of 10,000 m^3 without snow entrainment does not reach the Eigergletscher railway station.
- In **scenario 2** an ice avalanche with a volume of 10,000 m^3 entrains around 50,000 m^3 of snow. The avalanche core flows past the railway station at a lateral distance of 80 m (Fig. 7). However the powder cloud hits the railway station. The maximal impact pressure of the powder cloud is 10 kPa at the eastern end and decays rapidly to < 1 kPa. The nearly 40 m high powder cloud only overflows the Rotstock ridge locally.
- The simulation results of **scenario 3**, when an icefall with a volume of 80,000 m^3 breaks off without snow entrainment, are very similar to scenario 2. The core of the avalanche flows past the railway station at a lateral distance of 20 m and the impact pressure of the powder cloud decays from 10 to 0.5 kPa near the railway station. The ice avalanche reaches the area of the railway station 40 s after break-off.
- For the extreme **scenario 4** with an ice volume of 80,000 m^3 and unstable snow conditions the railway station is heavily endangered by the avalanche core and the powder cloud (Fig. 7). The ice avalanche entrains around 125,000 m^3 of snow. The calculated suspension ratio of the avalanche is nearly 15%. The mean height of the powder cloud is over 50 m. A part of the core of the avalanche flows over the Rotstock ridge. The core of the avalanche strikes a small area of the railway station with an impact pressure of up to 100 kPa. The simulations indicate that maximal impact pressures of the powder cloud > 50 kPa are possible. RAMMS probably calculates too high impact pressures of the powder cloud for scenario 4. The impact pressures were therefore adjusted, based on expert assumptions. The simulation results were an important input to the development of the closure plans for the investigated scenarios.

6. Closure plans

Based on the hazard assessment of the four scenarios we elaborated the closure plans A, B and C as part of the safety concept (see below and Fig. 8). Four different zones with varying impact pressures are defined for each plan. The red zone is reached by the core of the avalanche with impact pressures of over 30 kPa. The dark blue zone is hit with powder cloud impact pressures varying between 5 and 10 kPa and in the light blue zone the impact pressure decreases from 5 to 2 kPa. In the blue zones, a railway car can be overturned or doors and windows can break due to the impact pressure. In the yellow zone, the impact pressure of the powder cloud decays from 2 to 0.5 kPa. We consider an impact pressure of 0.5 kPa as a lower limit for unprotected people.

Consequently, the necessary safety measures for all buildings, locations and infrastructure in the area of the railway station Eigergletscher were determined in relation to the different zones of the closure plans A, B and C. If for example closure plan B (Fig. 8) is operative, the railway station and a ski run are closed to the public and a specific type of railway wagons are used.

7. Safety measures

The safety concept determines temporary safety measures for the different closure plans depending on the volume of an impending icefall from the hanging glacier in combination with the amount of erodible snow (Fig. 9). We recommended to install an early warning and alarm system as a basis for the safety concept (Sättele and Bründl, 2015), in order to detect an impending icefall in time and to minimize the closure times for the railway and ski area. An **early warning system** measures precursors of an event, in this case a local acceleration of the glacier surface velocity. In contrast, an **alarm system** detects the event itself in real time, i.e. the break-off of an ice lamella and the subsequent formation of an avalanche. A survey of the hanging glacier based on visual observations and interpretation of photos taken by an automatic camera were considered to be insufficient because neither the volume nor the timing of a break-off could be determined reliably, especially during periods of bad visibility.

A monitoring system consisting of a Ground-Based Interferometric Synthetic Aperture Radar (GB-InSAR) and a Doppler radar, as well as several webcams was installed in February 2016 (Meier et al., 2016). The radars are located at the railway station, at a line-of-sight distance of 1.8 km from the hanging glacier (Fig. 10). The vertical elevation difference between the radar and the glacier is around 1000 m.

GB-InSAR is widely used to monitor surface deformation in open-pit mines or for assessing slope instabilities and landslides (e.g. Monserrat et al., 2014). The radar device emits radiation with a frequency of around 17 GHz towards the target area and records the signal reflected from the target. Phase differences of the received signal of two radar acquisitions are analysed. After compensating for phase changes induced by varying atmospheric conditions, the phase difference is proportional to the deformation of a target pixel between the two measurements. Modulating the transmission frequency enables range resolution, usually in the order of 1 m, depending on the allowed frequency bandwidth. Azimuth resolution can be achieved by rotating antennas (Werner et al., 2008) or by consecutively acquiring radar scans along a linear stage, forming a synthetic aperture (e.g. Rödelsperger, 2011). Pixels with good reflective properties within the area of interest are extracted and sent to a processing server that removes the atmospheric influences and overlays the derived deformation map onto a digital terrain model (Fig. 11). If the data quality is considered good by an algorithm on this server, the deformation maps are uploaded once an hour to a password-protected internet site for interpretation by glaciologists. Snow fall or snow drift as well as rain or a strong atmospheric variability can temporarily lead to a high level of noise in the data, making the interpretation of the deformation maps difficult or even impossible. Under normal conditions, one good measurement per day is considered sufficient. According to this definition, the system had an availability of 95% during the 266 days of operation between February 2016 and November 2016: The system worked flawlessly on all of those days. However, for 14 days, the automatic algorithms did not consider any data good enough to be automatically uploaded to the online platform. During that period, the data had to be interpreted manually by radar specialists to estimate relevant glacier deformations.

The deformation map (Fig. 11) allows estimating the unstable ice volume and the surface velocities. The most promising approach to predict an icefall is based on the distinct acceleration of the unstable ice volume prior to break-off (Pralong and Funk, 2006). The surface velocities are analysed manually by glaciologists every morning. If the surface velocity exceeds 0.15 m d^{-1} and if acceleration is observed a critical situation can develop. In practice a critical velocity of 0.4 m d^{-1} is often suggested to determine the time period of highly likely break-off occurrence (Faillettaz et al., 2016). The maximal surface velocity at the front of the hanging glacier on the Eiger W-face is generally below 0.05 m d^{-1} which is considered as non-critical. Additionally, the surface displacements on the glacier front are assessed to estimate the volume of an unstable ice lamella.

The stability of the snow cover and the amount of erodible snow is evaluated in winter by the safety service of the Jungfrau Railways. An erodible snow depth of 0.4 m is considered as the lower limit for which an ice avalanche can entrain relevant snow masses. If possible, avalanches are triggered artificially by helicopter blasting below the hanging glacier to reduce the amount of erodible snow. Based on this information and with the help of a decision tree (Fig. 12), the necessary safety measures and the closure plan to be applied are determined.

Data from the GB-InSAR system were used as a basis for the decision to close a ski run, a restaurant terrace and part of the railway station

Eigergletscher for several days before an expected event. The train services should preferably not be halted for such an extended period of time because of the high economic loss. Therefore for the trains and a construction site close to the tunnel portal, an alarm system operating with a Doppler radar was installed.

The Doppler radar detects releasing ice and/or snow avalanches around the clock and in all weather conditions and automatically triggers an alarm. Like the GB-InSAR, it can detect the range and azimuth of movements in its field of view that covers 90° horizontally and 10° vertically. In contrast to GB-InSAR, it analyses frequency changes (Doppler shift) and detects moving targets in real time. All movements of objects reflecting enough radar radiation are detected such as skiers, birds, helicopters or avalanches. A proprietary algorithm selects movements that look like avalanches and estimates their size. The system sounds an alarm and activates stop lights in the tunnel and the railway station if an avalanche of a certain minimum size is detected below the glacier. Given a warning time of 35 to 45 s, both people and trains can move to safety, for example into the tunnel if they are in the danger zone when the avalanche is detected. The alarm system also allows a safe operation of the railway if closure plan B is activated. The Doppler radar is only operated in winter time.

In winter 2016 three icefalls (3 March, 7 April and 12 April 2016) were recognized one to a few days in advance by manually analysing the velocity time series. Shortly before failure, the displacement velocities were higher than 0.4 m d^{-1} and the active area on the glacier front was smaller than 200 m^2 (Figs. 11 and 13). Because the ice volumes were smaller than 10,000 m^3 and the snow cover was sufficiently stable, no closure plan had to be activated. The icefalls did not entrain much snow and the powder cloud caused negligible impact pressures in the area of the railway station. The icefalls were successfully detected with the Doppler radar system (Fig. 14) but because no closure plan was active, the alarm was suppressed.

A surprising number of 606 avalanches were detected between 24 February 2016 and 5 June 2016 in the west face of the Eiger. Most avalanches were rather small and occurred after snowfalls or during warming periods. The avalanches usually stopped at the base of the rock faces in the potential trigger zone for secondary snow avalanches. This sluffing activity seems to disturb and stabilize the snowpack so that the probability of secondary avalanche releases is reduced. On April 10, 2016 > 15 avalanches were recorded (see video GEOPRAEVENT, 2016).

Finally, we proposed to elongate the lower end of the tunnel to the Jungfraujoch by a 45 m long snow shed so that the railway can no longer be hit by the core in scenario 4. Based on the RAMMS simulations, we determined the avalanche actions on the planned snow shed.

8. Conclusions

The established safety concept that is based on closure maps and an early warning and alarm system allows to operate the railway to the Jungfraujoch at an acceptable risk level despite the imminent danger of ice avalanches. The installed GB-InSAR has detected several detachments of ice lamellas from the Eiger hanging glacier a couple of days in advance. A decision tree was developed to determine the required closure plan based on the interpretation of radar signals and information on the snowpack stability. Thanks to the Doppler radar it is possible to keep the trains to the Jungfraujoch running safely, as the radar automatically detects larger avalanches and the trains can be stopped in safe places.

In this study, we applied the research version of RAMMS, a two-layer numerical avalanche dynamics model, to analyse the hazard of ice avalanches breaking off the Eiger hanging glacier. RAMMS simulations were very helpful to quantify the differences between the four investigated scenarios and to establish detailed closure plans. The interaction of ice avalanches with the snowpack is particularly challenging and still poorly understood as there is a lack of good field data. The monitoring of ice avalanches with a GB-InSAR and Doppler radar may contribute to a better understanding of this process.

In summary, we think that the safety concept including closure plans based on an avalanche dynamics study and on measurements with GB-InSAR and Doppler radars can be considered as state-of-the-art technology for managing the risk of ice avalanches from hanging glaciers. This approach is particularly useful if there is relevant damage potential or if small ice volumes need to be detected because they may trigger secondary snow avalanches.

References

Bartelt, P., Buser, O., Vera, Valero C., Bühler, Y., 2016. Configurational energy and the formation of mixed flowing/powder snow and ice avalanches. Ann. Glaciol. 57 (71), 179–188.

Buser, O., Bartelt, P., 2015. An energy-based method to calculate streamwise density variations in snow avalanches. J. Glaciol. 61 (227). http://dx.doi.org/10.3189/2015JoG14J054.

Christen, M., Kowalski, J., Bartelt, P., 2010. RAMMS: numerical simulation of dense snow avalanches in three-dimensional terrain. Cold Reg. Sci. Technol. http://dx.doi.org/10.1016/j.coldregions.2010.04.005.

Faillettaz, J., Sornette, D., Funk, M., 2011. Numerical modeling of a gravity-driven instability of a cold hanging glacier: reanalysis of the 1895 break-off of Altelsgletscher, Switzerland. J. Glaciol. 57 (205), 817–831. http://dx.doi.org/10.3189/002214311798043852.

Faillettaz, J., Funk, M., Vincent, C., 2015. Avalanching glacier instabilities: review on processes and early warning perspectives. Rev. Geophys. 53 (2), 203–224.

Faillettaz, J., Funk, M., Vagliasindi, M., 2016. Time forecast of a break-off event from a hanging glacier. Cryosphere 10, 1191–1200. http://dx.doi.org/10.5194/tc-10-1191-2016.

GEOPRAEVENT, 2016. Alle Lawinen Eigergletscher on 19 April 2016. https://youtu.be/Zo66mNTXqag (Retrieved from, Web. 24 November 2016).

Gilbert, A., Gagliardini, O., Vincent, C., Wagnon, P., 2014. A 3-D thermal regime model suitable for cold accumulation zones of polythermal mountain glaciers. J. Geophys. Res. Earth Surf. 119, 1876–1893. http://dx.doi.org/10.1002/2014JF003199.

Huss, M., Fischer, M., 2016. Sensitivity of very small glaciers in the Swiss Alps to future climate change. Front. Earth Sci. 4, 34. http://dx.doi.org/10.3389/feart.2016.00034.

Lüthi, M., Funk, M., 1997. Wie stabil ist der Hängegletscher am Eiger? In: Spektrum der Wissenschaft. 5. pp. 21–24.

Margreth, S., Faillettaz, J., Funk, M., Vagliasindi, M., Diotri, F., Broccolato, M., 2011. Safety concept for hazards caused by ice avalanches from the Whymper hanging glacier in the Mont Blanc massif. Cold Reg. Sci. Technol. 69, 194–201. http://dx.doi.org/10.1016/j.coldregions.2011.03.006.

Meier, L., Jacquemart, M., Blattmann, B., Wyssen, S., Arnold, B., Funk, M., 2016. Radar-based warning and alarm systems for alpine mass movements. In: Proceedings of INTRAPRAEVENT 2016, 30 May-2 June, Lucerne, Switzerland, pp. 960–968.

Monserrat, O., Corsetto, M., Luzzi, G., 2014. A review of ground-based SAR interferometry for deformation measurement. ISPRS J. Photogramm. Remote Sens. 93, 40–48.

Pralong, A., Funk, M., 2006. On the instability of avalanching glaciers. J. Glaciol. 52 (176), 31–48. http://dx.doi.org/10.3189/172756506781828980.

Pralong, A., Birrer, C., Stahel, W.A., Funk, M., 2005. On the predictability of ice avalanches. Nonlinear Process. Geophys. 12, 849–861.

Raymond, M., Wegmann, M., Funk, M., 2003. Inventar gefährlicher Gletscher in der Schweiz, VAW Mitteilungen 182, Herausgeber: Prof. Dr. Ing H.-E. Minor.

Rödelsperger, S., 2011. Real-time Processing of Ground Based Synthetic Aperture Radar (GB-SAR) Measurements. Verlag der Bayerischen Akademie der Wissenschaften in Kommission beim Verlag. C.H. Beck, München.

Sättele, M., Bründl, M., 2015. Praxishilfe für den Einsatz von Frühwarnsystemen für gravitative Naturgefahren. Davos, WSL-Institut für Schnee- und Lawinenforschung SLF; Bern, Bundesamt für Bevölkerungsschutz/BABS. 61 S.

Werner, C., Strozzi, T., Wiesmann, A., Wegmüller, U., 2008. Gamma's portable radar interferometer. 13th FIG Symposium on Deformation Measurements ad Analysis, LNEC, Lisbon May 12–16 2008.